

# Solutions of hybrid silica microgels as precursors of sol–gel coatings

Sergio A. Pellice,<sup>ac</sup> Roberto J. J. Williams,<sup>a</sup> Isabel Sobrados,<sup>b</sup> Jesús Sanz,<sup>b</sup> Yolanda Castro,<sup>c</sup> Mario Aparicio<sup>c</sup> and Alicia Durán<sup>\*c</sup>

Received 20th April 2006, Accepted 20th June 2006

First published as an Advance Article on the web 12th July 2006

DOI: 10.1039/b605693h

A two-step process to synthesize a new type of organic–inorganic hybrid sol, that may be used for a variety of processes related to sol–gel chemistry, is analyzed. The first step consisted of a typical inorganic polycondensation of tetraethoxysilane (TEOS) and 3-methacryloxypropyl-trimethoxysilane (MPMS) leading to a conventional sol. In the second step a convenient amount of a solvent (isopropanol), and a vinyl co-monomer (2-hydroxyethylmethacrylate, HEMA) were added. The free-radical co-polymerization of the C=C groups of MPMS and those of the co-monomer was carried out by using a suitable initiator (2,2'-azobis(isobutyronitrile), AIBN). The advance in the organic and inorganic polymerizations was followed employing different experimental techniques: FTIR, <sup>13</sup>C NMR, <sup>29</sup>Si NMR and viscosity measurements. The key to the new process was the amount of solvent added before the second stage such that gelation did not occur after complete consumption of C=C groups. This led to a solution of hybrid microgels (a hybrid sol) that was characterized by scanning electron microscopy (SEM) and exhibited the following characteristics: a) it could be stored for prolonged periods at room temperature without gelation, b) it led to extremely fast gelation by solvent evaporation and c) it had a high wettability that allowed the production of coatings over different substrates. Besides, in this new process it is possible to add co- and ter-monomers in the second step to provide a desired functionality to the resulting coating. These concepts may be used to synthesize a variety of sols for the extended field of sol–gel processes.

## Introduction

Hybrid organic–inorganic materials have won interest in the current marketplace, with one of the most important applications being their use as coating films.<sup>1–3</sup> Different types of formulations may be employed to synthesize a hybrid coating. Following the classification of Sanchez and Ribot,<sup>4</sup> hybrids of class II are those exhibiting covalent bonding between the organic and inorganic components. Hereafter the analysis will be focused on the subclass where the organic and inorganic parts have polymerizable groups. These materials develop organic and inorganic networks whose extension and configuration are mutually dependent.<sup>5</sup>

The polymerization of organic and inorganic precursors may be carried out sequentially or simultaneously.<sup>6,7</sup> Examples where the organic polymerization is performed first are based on the synthesis of linear polymers or copolymers that are functionalized with precursors of the inorganic polymer like trialkoxysilane groups, present either in the polymer backbone

or at chain ends.<sup>8–10</sup> An inconvenience of starting with the organic polymerization is the relatively high viscosities of the resulting solutions and the need to prevent contact with humidity to avoid gelation of the hybrid precursors.

Most frequently, films are formed through conventional sol–gel processes in which the inorganic polymerization is first started in the sol stage, the coating is formed and both the organic and inorganic polymerizations are then produced in the coated material. However, it is difficult to advance both organic and inorganic networks to high conversions due to the steric restrictions imposed by the covalent bonds between them. An adequate tuning of initial formulations and reaction conditions has been recently proposed to obtain high conversions in both polymerizations.<sup>5,11</sup> The use of a high fraction of a tetraalkoxysilane in the formulation leads to an inorganic network with a rigid silica backbone that does not allow the organic polymerization to take place.<sup>5</sup> On the other hand, the use of a low fraction of an organic co-monomer leads to an incomplete conversion of the organic polymer network.<sup>12–14</sup>

The aim of this study was to investigate the feasibility of synthesizing a new type of organic–inorganic hybrid sol based on solutions of microgels, an approach that is employed to decrease the viscosity of UV-cure formulations used to produce organic coatings. In this field, the decrease in viscosity is achieved by the use of solutions of crosslinked polymer microparticles (microgels) bearing reactive functionalities.<sup>15–19</sup> Microgels can be described as polymer particles with sizes in the submicrometer range with permanent shape, surface area, and solubility. The use of dispersion/emulsion aqueous or

<sup>a</sup>Instituto de Investigaciones en Ciencia y Tecnología de Materiales (INTEMA), Universidad Nacional de Mar del Plata–CONICET, J. B. Justo 4302, 7600 Mar del Plata, Argentina.

E-mail: serpell@fi.mdp.edu.ar; Fax: +54 223 4810046; Tel: +54 223 4816600

<sup>b</sup>Instituto de Ciencia de Materiales de Madrid (CSIC), Campus de Cantoblanco, 28049 Madrid, España. E-mail: jsanz@icmm.csic.es; Fax: +34 91 3720623; Tel: +34 91 3721420

<sup>c</sup>Instituto de Cerámica y Vidrio (CSIC), Campus de Cantoblanco, 28049 Madrid, España. E-mail: aduran@icv.csic.es; Fax: +34 91 7355843; Tel: +34 91 7355840

nonaqueous formulations containing adequate concentrations of multifunctional monomers is the most controllable way of manufacturing microgel-based systems.<sup>16</sup> The sizes of microgels prepared in this way vary between 50 and 300 nm. Functional groups are either distributed in the whole particle or are grafted onto the surface. Due to their compact structure, microgels significantly decrease viscosity with respect to linear polymers and a high microgel concentration can be used without a significant increase in the solution viscosity. This is a relevant property for the potential use of solutions of hybrid organic–inorganic microgels in the synthesis of coatings by the sol–gel process (the term “solution of microgels” may be questioned; however, we will keep this denomination throughout the text on the basis that every microgel particle is an individual high-molar mass molecule surrounded by solvent molecules).

The desired hybrid microgels should contain residual silanol (SiOH) or alkoxy silane groups (SiOR) to produce a fast gelation by solvent evaporation but the solution should be stable for a prolonged period at room temperature. The organic part should be fully polymerized to avoid the presence of residual monomers in the final coating (or the need to polymerize them). Therefore, the key to obtaining this product is how to convey the organic polymerization of multifunctional monomers to full conversion avoiding gelation.

The formulation selected to illustrate the feasibility of the process was based on three components: 2-hydroxyethyl methacrylate (HEMA), 3-methacryloxypropyltrimethoxysilane (MPMS), and tetraethoxysilane (TEOS), with chemical structures shown in Fig. 1. MPMS was the coupling monomer between the organic and inorganic networks. The synthesis was carried out in a two-step process. Hydrolysis and condensation of MPMS and TEOS were advanced in a first stage leading to a sol containing molecules bearing multiple C=C bonds (oligomers composed of MPMS and TEOS units joined through Si–O–Si bonds). In a second stage HEMA and extra solvent were added to the sol resulting from the first stage, and the organic free-radical polymerization was launched using a typical initiator. The questions that we address in this study are: *a*) is it possible to drive the organic polymerization to the formation of a stable solution of microgels with 100% conversion of C=C bonds? And *b*), if this is possible, has the resulting sol the capability of forming crosslinked films by the continuation of the inorganic

polymerization after solvent evaporation? A positive answer to both questions will open a new way for the synthesis of organic–inorganic hybrid coatings.

## Experimental

### Materials

The precursor sol was synthesized employing 2-hydroxyethyl-methacrylate (HEMA, Aldrich, 97%), 3-methacryloxypropyl-trimethoxysilane (MPMS, ABCR, 98%), and tetraethoxysilane (TEOS, ABCR, 98%), used without further purification. A 0.1 N HNO<sub>3</sub> solution was used as catalyst. The initiator of the organic polymerization was 2,2'-azobis(isobutyronitrile) (AIBN, Aldrich, 98%). Isopropanol (Panreac, analytical grade) was employed as solvent.

### Synthesis of sols

Sols were synthesized following a two-step process. In the first step, a solution of appropriate amounts of TEOS, MPMS and HNO<sub>3</sub> 0.1 N in isopropanol was formed at a Si concentration of 70 g L<sup>-1</sup>. Hydrolysis and condensation reactions were produced at 50 °C for 3 h in a closed reactor. The amount of water supplied by the 0.1 N HNO<sub>3</sub> solution was the stoichiometric amount required for producing complete hydrolysis and condensation through formation of Si–O–Si bonds (2 moles per mol of TEOS and 1.5 moles per mol of MPMS). In the second step, appropriate amounts of HEMA and AIBN were added to the pre-condensed sol together with an extra amount of isopropanol to reach the concentrations indicated in Table 1. The amount of AIBN was 0.01 moles per mol of C=C groups. The organic polymerization was carried out at 65 °C in a closed reactor. Samples (about 15 mL) were extracted from the reactor at different reaction times and rapidly cooled to 5 °C to stop the organic and inorganic polymerization. These samples were used to monitor the evolution of the conversion and the viscosity of the sol as a function of time.

Hybrid sols synthesized from TEOS, MPMS and HEMA will be denoted as TMH sols. The Si concentration, expressed in g L<sup>-1</sup>, is included in the notation as TMH-19, TMH-26 and TMH-33. For comparison purposes, sols containing only TEOS and MPMS, denoted as TM sols, or TEOS and HEMA, indicated as TH sols, were also synthesized. Molar ratios of monomers, water and initiator of the different sols, Si and initial C=C concentrations in the isopropanol solution are given in Table 1. The behaviour of TMH sols was compared on the basis of their Si concentration in the isopropanol solution while the comparison of TMH, TM and TH sols was

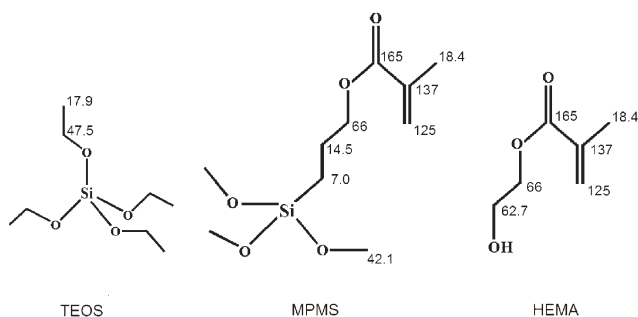


**Fig. 1** Chemical structures of HEMA, MPMS and TEOS. <sup>13</sup>C NMR chemical shifts values (ppm) of different groups are included in this representation.

**Table 1** Molar ratios of monomers, water and initiator of the different sols and Si and initial C=C concentrations in the isopropanol solution

Sol	TEOS	MPMS	HEMA	H <sub>2</sub> O	AIBN	Si/g L <sup>-1</sup>	[C=C] <sub>0</sub> /mol L <sup>-1</sup>
TMH-19	0.60	0.10	0.30	1.35	0.004	19	0.38
TMH-26	0.60	0.10	0.30	1.35	0.004	26	0.52
TMH-33	0.60	0.10	0.30	1.35	0.004	33	0.67
TM	0.60	0.40	0	1.80	0.004	36	0.52
TH	0.60	0	0.40	1.20	0.004	22	0.52

made keeping constant the concentration of C=C groups in the initial solution.

### Viscosity

The evolution of the viscosity of different sols, during the second stage of the synthesis, was measured at 25 °C and at a shear rate of 1000 s<sup>-1</sup> using a rotational rheometer (Haake, RS50, Germany) provided with a cone and a plate fixture (5 mL samples). The shear rate was increased from 0 to 1000 s<sup>-1</sup> in 5 min, kept for 1 min at the maximum rate and decreased again to 0 in 5 min.

### FTIR spectroscopy

Fourier transform infrared spectroscopy was used to study the hydrolytic Si–O–Si condensation during the first stage of the synthesis and the evolution of the C=C groups during the second stage in liquid samples. The evolution of bands involved in the hydrolytic condensation of the first stage of synthesis was analyzed by attenuated total reflectance (FTIR Vertex 70, Brücker, with ATR-Golden Gate Specac) on liquid samples. To follow the conversion of C=C bonds, microdroplets were placed between KRS5 crystals (TlBr/TlI) and analyzed in transmission mode (FTIR 1760X, Perkin-Elmer). IR spectra were recorded between 400 and 4000 cm<sup>-1</sup>, with a resolution of 2 cm<sup>-1</sup>. Spectra were deconvoluted through a Levenberg Marquardt algorithm using software OPUS Version 5.5 from Vertex 70 Standard Systems. Best fits were performed considering Gaussian–Lorentzian 60:40 bands approximately. Bandwidths were kept between 20 and 30 cm<sup>-1</sup> while wavenumbers and intensities were allowed to vary. Residual RMS errors were around 0.001.

### NMR spectroscopy

<sup>13</sup>C and <sup>29</sup>Si solid state NMR spectra were obtained with a Bruker AVANCE 400 pulse spectrometer operating at 100.63 and 79.49 MHz, respectively, in presence of a 9.4 T magnetic field. Powder samples were prepared by solvent evaporation of partially reacted samples in a vacuum chamber at room temperature. MAS-NMR spectra were recorded after irradiation of samples with  $\pi/2$  pulses (6  $\mu$ s). Spinning rates used in MAS experiments were 10 kHz. In <sup>13</sup>C CP-MAS experiments, the contact time used in the Hartman–Hann condition was 2 ms. Times between scans were 30 s in <sup>29</sup>Si MAS, 10 s in <sup>13</sup>C MAS and 2 s in CP-MAS experiments. In all cases the number of scans was 400. Chemical shifts were referenced to external TMS. <sup>29</sup>Si liquid NMR spectra were performed on samples at the end of the first stage of synthesis under the same recording conditions used in the solid samples.

### SEM Characterization

The presence of microgels in the sol TMH-19 was confirmed by scanning electron microscopy (SEM, Jeol 6460). The samples were prepared by diluting the sol to a Si concentration of 0.28 g L<sup>-1</sup> by adding isopropanol, then a small droplet was deposited on a glass substrate and the solvent evaporated at room temperature; finally, prepared films were covered with a 8 nm thickness gold layer.

### Coatings

Coatings were obtained on glass and metallic (AISI 304 stainless steel and aluminium AA 3033) substrates by a conventional dip-coating process at withdrawal rates between 5 and 50 cm min<sup>-1</sup>. In this process the viscosity of the sol was adjusted with isopropanol addition to control the thickness of the coating.

### Results

The synthesis of sols was divided into two stages. The aim of the first stage was to advance the inorganic condensation reactions, leading to a pre-condensed sol. The purpose of the second stage was to investigate conditions that ideally enabled complete organic polymerization without gelation (generation of a solution of microgels).

### FTIR characterization

In the first stage of synthesis the process of hydrolytic condensation was followed by FTIR spectra. Fig. 2 shows the evolution of such bands at three consecutive times: *a*) before the addition of water, *b*) just after addition of water and *c*) after 5 minutes of thermal treatment of the sol at 50 °C. The deconvolution of the first spectra (Fig. 2*a*) in the region 850–1250 cm<sup>-1</sup> discriminates the main bands of isopropanol (at 950, 1109, 1128 and 1160 cm<sup>-1</sup>) from Si–O–R vibration of the alkoxides at  $\sim$ 1078 and 961 cm<sup>-1</sup> (bands 1 and 2, respectively). Just after water addition, the corresponding band of water appears at 1650 cm<sup>-1</sup> (band 3). In this spectrum, Fig. 2*b*, the bands of ethanol (produced by hydrolytic condensation of TEOS), Si–O–Si, Si–O<sup>-</sup> fragments and Si–OH,<sup>20</sup> are already present confirming that hydrolysis and condensation processes develop almost simultaneously with water addition. Ethanol presents three strong bands at 1088, 1046 and 880 cm<sup>-1</sup>; the last one being assigned to the methyl and methylene rocking modes (band 4), while the others are

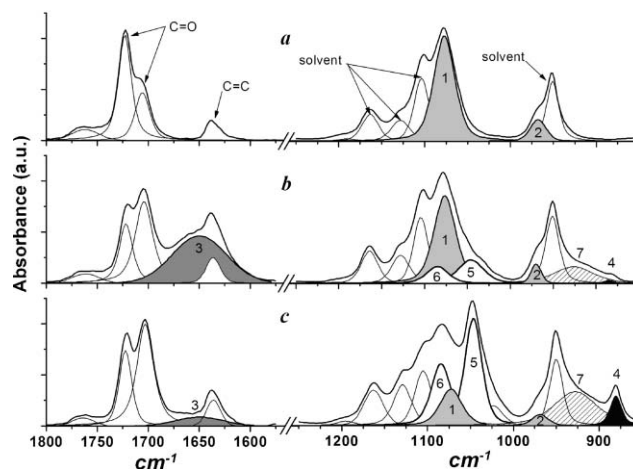


**Fig. 2** Evolution of FTIR spectra during the first stage of synthesis: *a*) before addition of water, *b*) after addition of water and *c*) after 5 minutes of thermal treatment at 50 °C. Deconvoluted bands of Si–O–R (1 and 2), H<sub>2</sub>O (3), ethanol (4), Si–O–Si (5 and 6), and Si–O<sup>-</sup> (7) are indicated.

overlapped with the vibration modes of Si–O–Si; at 1048 cm<sup>-1</sup> (band 5) and 1085 cm<sup>-1</sup> (band 6), both assigned to transversal optic (TO) modes, corresponding to different structural units (4-fold rings) with smaller siloxane rings, larger Si–O–Si angles and Si–O bond lengths.<sup>20,21</sup> Similar behaviour is observed with the corresponding band of Si–OH at 950 cm<sup>-1</sup>, which overlaps with the main band of isopropanol. A wide band appears at ~920 cm<sup>-1</sup> (band 7), that is usually assigned to Si–O<sup>-</sup> fragments present in primary silica particles.<sup>22</sup> After just 5 minutes of reaction at 50 °C the intensity of the water band decreases dramatically, Fig. 2c, showing the fast water consumption produced during hydrolysis. Consistently, Si–O–Si, Si–O<sup>-</sup> and ethanol bands grow at the expense of the Si–O–C bands of TEOS and MPMS, indicating a large extent of hydrolysis. The spectrum after 3 h of reaction (not shown in Fig. 2) revealed slight changes compared with the sample analysed after 5 minutes of reaction: decreasing of Si–O–R and Si–O<sup>-</sup> bands and increasing ethanol and Si–O–Si bands. Since water is added in stoichiometric ratio, the progress of condensation is required to generate the water necessary to complete the hydrolysis. The existence of residual Si–O–R and Si–OH groups indicates that hydrolysis and condensation reactions are not totally completed at the end of the first stage.

In the second stage of synthesis, the decrease in the concentration of C=C groups was also followed by FTIR spectroscopy. Fig. 3 shows FTIR spectra of the TMH-19 formulation, recorded between 1550 and 1850 cm<sup>-1</sup> at different reaction times. The intensity of the C=C band at 1639 cm<sup>-1</sup> decreases continuously and practically disappears at 70 h reaction. The C=O band has three different components:<sup>5</sup> a band at 1705 cm<sup>-1</sup> assigned to C=O hydrogen-bonded to OH groups of HEMA or to SiOH groups generated in the first stage, a band at ~1720 cm<sup>-1</sup> assigned to C=O stretching vibrations that are conjugated to C=C double bonds, and a band at 1732 cm<sup>-1</sup> assigned to C=O stretching vibrations, produced during the organic polymerization, that are not conjugated to C=C double bonds. According to these assignments, the organic polymerization generates the observed shift of the C=O band to larger wavenumbers. Thus, C=O bands are not appropriate references for quantitative evaluation of the C=C

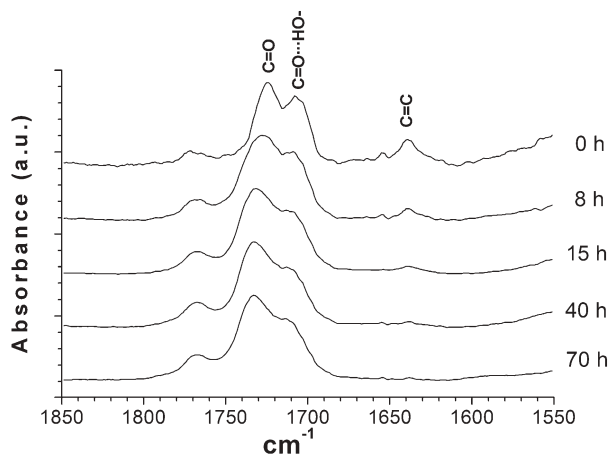


**Fig. 3** Evolution of FTIR spectra in the 1550–1850 cm<sup>-1</sup> range during the second stage of the synthesis of the TMH-19 sol.

conversion. However, these bands are useful for estimating the conversion degree through the ratio between the C=C band area with respect to the sum of the C=O band areas.

### NMR characterization

<sup>29</sup>Si MAS-NMR spectra were used to estimate the condensation degree of TEOS and MPMS monomers. In this analysis, the relative intensities of the Q<sup>0</sup> to Q<sup>4</sup> environments [Si(OSi)<sub>n</sub>(OH)<sub>4-n</sub>; n = 0–4] and the T<sup>0</sup> to T<sup>3</sup> environments [Si(OSi)<sub>n</sub>(OH)<sub>3-n</sub>(R); n = 0–3] were determined by deconvolution of NMR spectra in terms of elementary Gaussian peaks. Chemical shifts corresponding to different environments have been extensively discussed in the literature.<sup>5,10,23–25</sup> The conversion in the inorganic polycondensation was estimated by calculating the average condensation degrees of TEOS (maximum value, n = 4) given by the expression:

$$n = I(Q^1) + 2 I(Q^2) + 3 I(Q^3) + 4 I(Q^4)$$

where  $I(Q^n)$  is the relative intensity of the Q<sup>n</sup> band.

Fig. 4 shows the evolution of the <sup>29</sup>Si NMR spectra after the first stage (measured in solution) and during the second stage of the synthesis (obtained after solvent evaporation) for the TMH-19 sol. The condensation degree of TEOS after the first stage was determined as n = 2.45. After 30 min reaction in the second stage, the condensation degree exhibited a small increase (n = 2.66). It is not possible to assess if this small increase was produced by the continuation of inorganic condensation reactions or in the process of solvent evaporation. After about 8 h reaction in the second stage, the condensation degree of TEOS increased to a final value close to n = 2.90 and then it remained almost constant within the experimental error of the determination.

Regarding the condensation of MPMS, the spectra were not adequate to obtain quantitative information. T<sup>2</sup> groups were present in significant concentrations at the beginning of the second stage while T<sup>3</sup> groups increased their relative concentration at longer times.

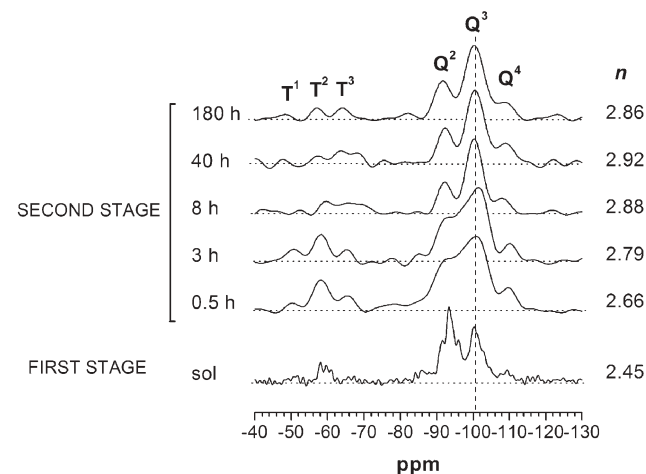


**Fig. 4** Evolution of <sup>29</sup>Si NMR spectra recorded during the second stage of the synthesis of the TMH-19 sol.



$^{13}\text{C}$  NMR spectra were used to obtain an estimation of the conversion of  $\text{C}=\text{C}$  bonds, that complements the estimation made by FTIR, during the second stage of the synthesis. Conversion was followed by monitoring the decrease of the intensity of the  $\text{CH}_2=\text{C}$  peak at 125 ppm and the  $\text{CH}_2=\text{C}$  peak at 137 ppm, and the increase in the intensity of the  $-\text{CH}_2-\text{C}-$  peak at 55 ppm and of the quaternary carbon  $-(\text{C}-)$  peak at 45 ppm.<sup>5,26</sup> The quantification was difficult because of the low initial intensity of the peaks at 125 and 137 ppm and the partial overlapping of peaks in the region between 40 and 70 ppm. A Gaussian deconvolution of peaks in the 40–70 ppm region was adopted to estimate the  $\text{C}=\text{C}$  conversion as the ratio between the intensity of the peak at 44 ppm with respect to the sum of intensities of the peaks at 60 ppm ( $-\text{CH}_2-\text{OH}$ ) and 66 ppm ( $-\text{CH}_2-\text{O}-\text{CO}$ ). A set of  $^{13}\text{C}$  NMR spectra recorded for TMH-19 samples after solvent evaporation is given in Fig. 5.

## Discussion

The synthesis of sols was carried out in two stages. After the first stage, the inorganic condensation produced a pre-condensed sol with a condensation degree of TEOS equal to  $n = 2.45$ , as deduced from the  $^{29}\text{Si}$  NMR spectrum. During the second stage, the organic polymerization progressed at a faster rate than the inorganic condensation (only a small increase in the average condensation degree of TEOS was observed during the second stage). Fig. 6 shows a schematic view of the chemical structure of the sol produced in the first stage. The relative amounts of  $\text{Q}^n$  and  $\text{T}^n$  groups of TEOS and MPMS are consistent with the  $^{29}\text{Si}$  NMR spectra.

The purpose of the second stage was to investigate conditions that enabled the complete polymerization of organic groups (generation of a solution of microgels) without producing macrogelation. The organic condensation produced during the second stage of reaction was analyzed with FTIR and NMR spectroscopies for TMH-19 samples. A large increase in the conversion of  $\text{C}=\text{C}$  groups took place during the first 24 h and the reaction was practically complete after about 48 h (Fig. 7).

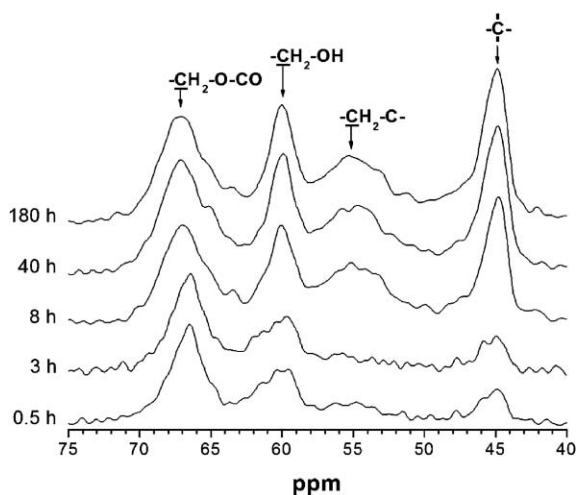


**Fig. 5** Evolution of  $^{13}\text{C}$  NMR spectra in the 40–75 ppm range during the second stage of the synthesis of the TMH-19 sol.

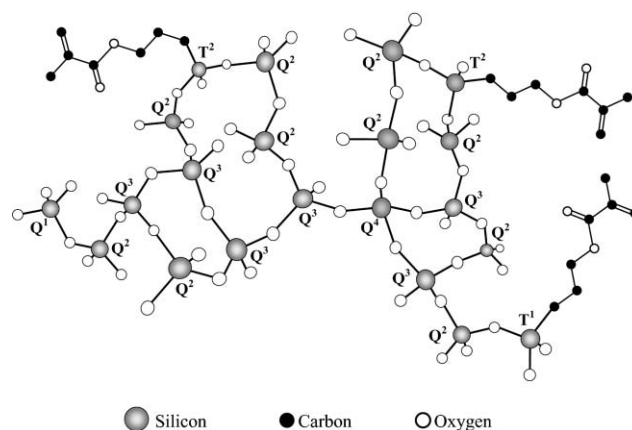


**Fig. 6** Schematic structures derived from relative amounts of  $\text{T}^n$  and  $\text{Q}^n$  NMR components. Oxygen atoms not bonded to Si atoms are bonded to H or to alkyl groups (not shown).

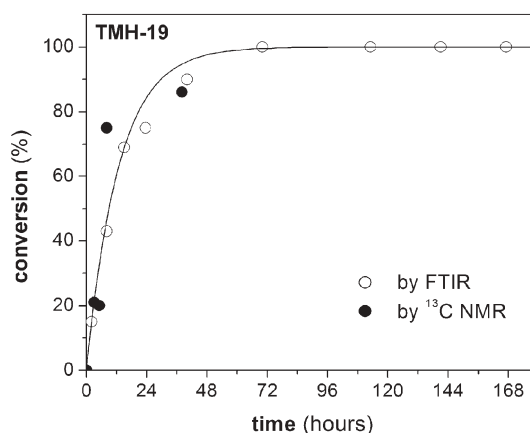


**Fig. 7**  $\text{C}=\text{C}$  conversion derived from FTIR and  $^{13}\text{C}$  NMR spectra of the TMH-19 sol.

In order to obtain direct proof of the existence of microgels, a sample of TMH-19 obtained after 5.5 h reaction during the second stage was diluted and analysed by SEM. For that, a small droplet was deposited over a glass substrate and covered with a fine gold layer after evaporating the solvent. Fig. 8 shows two regions of the sample at different magnifications. Isolated microgels, with sizes between 100 nm and 300 nm, are observed in Fig. 8a. Coalesced particles produced as a consequence of solvent evaporation are shown in Fig. 8b.

## Gelation

The evolution of the sol viscosity at 25 °C was followed during the second stage of the synthesis to determine gelation times of formulations TMH-19 (Fig. 9a), TMH-26 and TMH-33 (Fig. 9b). Gelation was observed at relatively short reaction times for the more concentrated solutions: at 2.5 h in TMH-33 and at 3.9 h in TMH-26. In the case of TMH-19, viscosity attained first a plateau at 48 h and then increased slowly leading to a gel at 180 h of reaction. In all these samples Newtonian behaviour was observed up to gelation. Two other sols, TM and TH (Table 1), were synthesized to discuss the

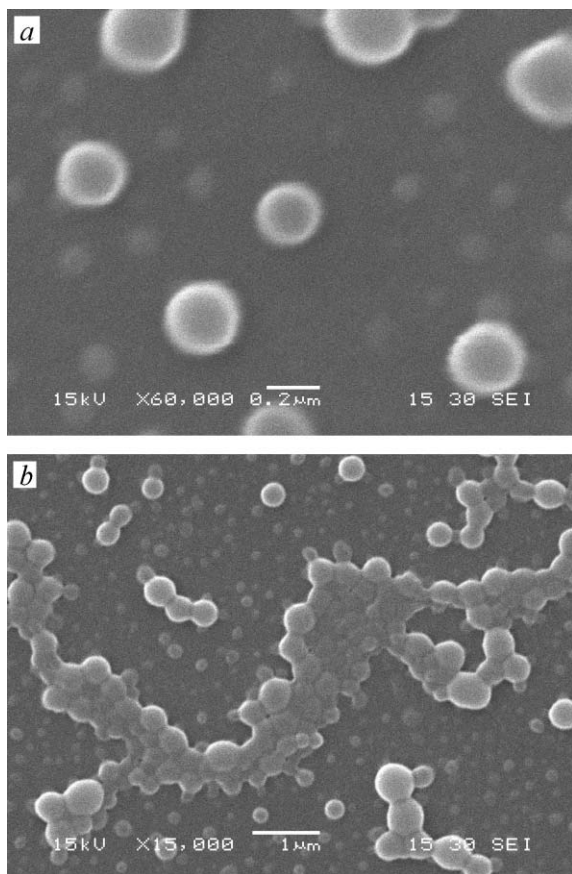


**Fig. 8** SEM micrographs of deposits produced over a glass substrate from the diluted TMH-19 sol: *a*) isolated microgels, *b*) partially coalesced microgels.

origin of gelation in the different formulations. While TM gelled after 4 h reaction, TH did not gel after 125 h.

Gelation is the point where the hybrid structure generated by both polymerizations percolates through the reaction medium. The necessary condition to produce gelation at a critical conversion is to polymerize monomers with a functionality higher than 2. In the inorganic polycondensation TEOS is a tetrafunctional monomer while MPMS is a trifunctional monomer. Therefore, gelation can occur by inorganic polycondensation if a critical value of the condensation degree ( $n$ ) is attained. In the sol-gel synthesis of silica by the acid-catalyzed hydrolysis and condensation of TEOS, the fractal dimension, density, and homogeneity of the gel depend strongly on reaction conditions such as the acid and water concentrations.  $^{29}\text{Si}$  NMR shows that gel conversions of at least 80% are observed over a wide range of initial acid ( $10^{-5}$ – $10^{-1}$  mol L $^{-1}$ ), water (4–22 mol L $^{-1}$ ), and TEOS (1.3–2.5 mol L $^{-1}$ ) concentrations.<sup>27</sup> The value of  $n$  to attain gelation (Table 2), corresponding to a conversion of 80%, is  $n = 3.20$  (usual values of gel conversion are 82–83% corresponding to  $n$  values close to 3.30).<sup>27</sup> If a fraction of TEOS (tetrafunctional) is replaced by MPMS (trifunctional), the value of  $n$  necessary to produce gelation should be even higher. For every formulation the following experimental values of  $n$  at the gel point were determined:  $n = 2.97$  for TM, 2.86 for TMH-19, 3.08 for TMH-26 and 3.10 for TMH-33.

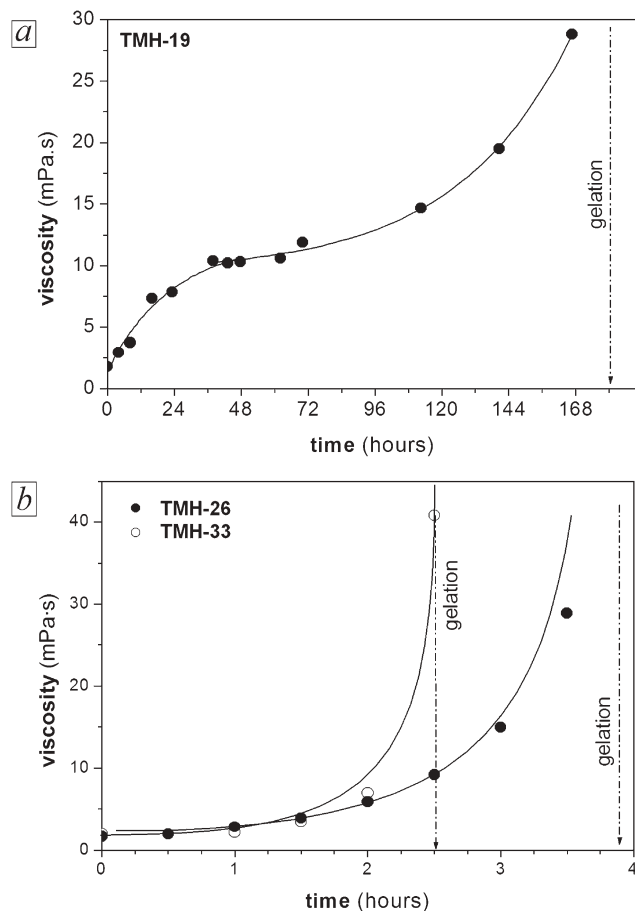


**Fig. 9** Evolution of the viscosity at 25 °C of: *a*) TMH-19, *b*) TMH-26 and TMH-33 sols, during the second stage of reaction.

**Table 2** Degrees of inorganic condensation ( $n$ ) and organic polymerisation ( $x$ ) at the moment of gelation ( $t_g$ )

Sample	$t_g$ /h	$n$	$x$ (%)
TMH-19	180	2.86	100
TMH-26	3.9	3.08	50
TMH-33	2.5	3.10	40
TM	4.0	2.97	45
TH	>125	—	100
TEOS	—	3.20 <sup>a</sup>	—

<sup>a</sup> Reference value taken from Ng *et al.*<sup>27</sup>

This means that the inorganic polycondensation alone was not responsible for the generation of a gel. For the sol TH after complete polymerization of HEMA (125 h) the condensation degree of TEOS was  $n = 3.06$  and the system had not yet gelled. In this case the organic polymerization did not contribute to gelation because HEMA is a bifunctional monomer.

Therefore, for every formulation the observed gelation was a result of both the inorganic and organic polymerizations. The inorganic polymerization took place mostly during the first stage of the synthesis and produced two main effects: *a*) it increased the average molar mass of species present in the sol approaching the system to gelation, and *b*) it generated species bearing multiple C=C groups per molecule provided by MPMS units (these species are multifunctional monomers for the

organic polymerization). The presence of these multifunctional monomers bearing multiple C=C groups explains why TM sol gelled by organic polymerization but TH sol did not gel even after complete consumption of C=C groups.

Now, turning the attention to TMH sols, after the first stage of the synthesis they are composed of a distribution of hybrid species bearing multiple C=C groups, a bifunctional co-monomer (HEMA), and an initiator that generates free radicals through thermal decomposition (AIBN). The difference among the studied formulations is the initial concentration of the solution in isopropanol. TMH-26 and TMH-33 are more concentrated than TMH-19, a fact that determined if the system did or did not gel by the organic polymerization. The free-radical polymerization produces chains formed by the covalent bonding of HEMA and MPMS units by reaction of their C=C groups. Units of MPMS incorporated into a polymer chain may belong to different molecular species of the sol obtained after the first stage of the synthesis (intermolecular reaction), or to the same molecule (intramolecular reaction). While intermolecular reactions contribute to the percolation of the hybrid structure and lead to gelation, intramolecular reactions only increase the size of individual macromolecules that remain dissolved in solution and do not produce a gel. The key to control the competition between inter- and intramolecular reactions is the initial dilution in the solvent. Increasing the dilution leads to an increase in the fraction of intramolecular reaction. For a critical dilution the system does not gel and a solution of hybrid microgels is obtained (the term microgel is used to indicate that there is percolation of the structure inside every particle). This is the explanation of the viscosity curves observed for the different TMH formulations. TMH-33 led to a gel at about 40% conversion of C=C groups while TMH-26 produced a gel at about 50% conversion of C=C groups. For TMH-19 the critical dilution was attained and the system did not gel after complete conversion of C=C groups (at about 48 h). For this formulation the increase in viscosity during this period should be related to the increase in the average size of the population of hybrid microgels. The plateau attained in viscosity (Fig. 9a) is practically coincident with the end of the organic polymerization (Fig. 7). However, the inorganic polycondensation continued slowly during the second stage of the synthesis binding microgel particles by the reaction of free SiOH and SiOR groups. This finally led to gelation after 180 h at the reaction temperature (65 °C). A similar process occurs at a much faster rate during preparation of films by solvent evaporation. Table 2 summarises the degrees of organic polymerisation and inorganic condensation at the gel point for each sol.

### Properties of TMH-19 sol

After achieving complete conversion of C=C groups (48 h of reaction), TMH-19 sols were used to obtain coatings over different substrates. An excellent wetting of glass and metallic substrates was produced; transparent and uniform hybrid films could be obtained by dip coating. The stability of the sol was checked by storing at 5 °C during 10 months. After this prolonged storage time, the sol retained the appearance of a

homogeneous solution without any sign of phase segregation. In general, sols bearing C=C conversions higher than 15% produced high-quality coatings. However, sols extracted from the reactor at very low conversions of organic groups exhibited poor wetting, leading to non-uniform films. Wetting problems have also been reported for hybrid formulations bearing a significant fraction of hydrophobic organic groups.<sup>28,29</sup>

In the formulation used in this work, HEMA supplies a hydrophilic C–OH group; however, the presence of this group was not enough to counterbalance the effect of hydrophobic organic chains if the reaction in the second stage was not advanced to a critical conversion, 15%. A possible explanation for wetting improvement, observed at advanced conversions, may be based on a nanostructuring at the level of microgel particles. Due to the dissolution of the microgels in a hydrophilic solvent (isopropanol), it should be expected that more hydrophilic groups (CH<sub>2</sub>OH, SiOH) are segregated to the surface of the microgels improving the wettability of the sol over different substrates. Therefore, the critical conversion where correct wettability is observed might be associated with the presence of an adequate amount of CH<sub>2</sub>OH groups of polymerized HEMA units at the surface of the microgels. Besides, in this new process it is possible to add co- and ter-monomers in the second step to provide a desired functionality to the resulting coating. These concepts may be used to synthesize a variety of sols for the extended field of sol–gel processes.

### Conclusions

The synthesis of a new class of organic–inorganic hybrid sols has been reported using a two-step process. The first step consisted of a typical inorganic polycondensation of TEOS and MPMS leading to a conventional sol. In the second step a convenient amount of a solvent (isopropanol), and a vinyl co-monomer were added (HEMA). The free-radical polymerization of the C=C groups of MPMS and those of a co-monomer was carried out by using a suitable initiator (AIBN). The key of the process was to control the initial dilution in such a way that gelation did not occur after complete conversion of C=C groups. This led to hybrid microgels with the following characteristics: *a*) it could be stored for prolonged periods, up to 10 months, at 5 °C without gelation and maintaining its rheological properties, *b*) it led to extremely fast gelation by solvent evaporation; *c*) the wettability over different substrates could be controlled by the conversion degree of C=C, which governs the microgel formation.

This process opens the possibility of adding co- and ter-monomers to provide desired functionalities to the resulting coatings, extending the field of sol–gel processes.

### Acknowledgements

The financial support from CONICET, ANPCyT and University of Mar del Plata (Argentina) as well as the Spanish projects MAT 2003-05902 and Ramón y Cajal (Ministerio de Ciencia y Tecnología) are gratefully acknowledged. The authors also thank Laura Pelaez for their assistance with the experimental techniques.

---

## References

- 1 B. Arkles, *Chemtech*, 1999, **29**, 12, 7.
- 2 D. A. Loy, *MRS Bull.*, 2001, **26**, 5, 364.
- 3 B. Arkles, *MRS Bull.*, 2001, **26**, 5, 402.
- 4 C. Sanchez and F. Ribot, *New J. Chem.*, 1994, **18**, 10, 1007.
- 5 P. Innocenzi, G. Brusatin, S. Licoccia, M. L. Di Vona, F. Babonneau and B. Alonso, *Chem. Mater.*, 2003, **15**, 4790.
- 6 U. Schubert, N. Hüsing and A. Lorenz, *Chem. Mater.*, 1995, **7**, 2010.
- 7 G. Kikelbick, *Prog. Polym. Sci.*, 2003, **28**, 1, 83.
- 8 Y. Wei, R. Bakthavatchalam and C. K. Whitecar, *Chem. Mater.*, 1990, **2**, 4, 337.
- 9 Y. Wei, D. Yang and L. Tang, *J. Mater. Res.*, 1993, **8**, 1143.
- 10 Y. Abe, Y. Honda and T. Gunji, *Appl. Organomet. Chem.*, 1998, **12**, 749.
- 11 P. Innocenzi, G. Brusatin, M. Guglielmi and R. Bertani, *Chem. Mater.*, 1999, **11**, 1672.
- 12 L. Delattre, C. Dupuy and F. Babonneau, *J. Sol–Gel Sci. Technol.*, 1994, **2**, 185.
- 13 M. A. Fanovich, S. A. Pellice, P. G. Galliano and R. J. J. Williams, *J. Sol–Gel Sci. Technol.*, 2002, **23**, 45.
- 14 P. Eisenberg, J. C. Lucas and R. J. J. Williams, *Macromol. Symp.*, 2002, **189**, 1.
- 15 L. J. Boggs, M. Rivers and S. G. Bike, *J. Coat. Technol.*, 1996, **68**, 63.
- 16 W. Funke, O. Okay and B. Müller, *J. Adv. Polym. Sci.*, 1998, **136**, 139.
- 17 J. P. Pascault, H. Sautereau, J. Verdu and R. J. J. Williams, *Thermosetting Polymers*, Marcel Dekker, New York, 2002.
- 18 L. Valette, J. P. Pascault and B. Magny, *Macromol. Mater. Eng.*, 2002, **287**, 41.
- 19 L. Valette, J. P. Pascault and B. Magny, *Macromol. Mater. Eng.*, 2003, **288**, 642.
- 20 A. Fidalgo and L. M. Ilharco, *J. Non-Cryst. Solids*, 2001, **283**, 144.
- 21 Z. Sassi, J. C. Bureau and A. Bakkali, *Vib. Spectrosc.*, 2002, **28**, 299.
- 22 A. Chmel, E. K. Mazurina and V. S. Shashkin, *J. Non-Cryst. Solids*, 1990, **122**, 285.
- 23 D. P. Fasce, R. J. J. Williams, F. Méchin, J. P. Pascault, M. F. Llauro and R. Pétaud, *Macromolecules*, 1999, **32**, 4757.
- 24 E. Lippmaa, M. Mägi, A. Samoson, G. Engelhardt and A. R. Grimmer, *J. Am. Chem. Soc.*, 1980, **102**, 4889.
- 25 G. Engelhardt and D. Michel, *High Resolution Solid State NMR of Silicates and Zeolites*, Wiley, New York, 1987.
- 26 F. Mammeri, E. Le Bourhis, L. Rozes and C. Sanchez, *J. Eur. Ceram. Soc.*, 2006, **26**, 259.
- 27 L. V. Ng, P. Thompson, J. Sanchez, C. W. Macosko and A. V. McCormick, *Macromolecules*, 1995, **28**, 6471.
- 28 S. Pellice, P. Galliano, Y. Castro and A. Durán, *J. Sol–Gel Sci. Technol.*, 2003, **28**, 81.
- 29 S. H. Messaddeq, S. H. Pulcinelli, C. V. Santilli, A. C. Wastaldi and Y. Messaddeq, *J. Non-Cryst. Solids*, 1999, **247**, 16.